

Thermal and Solutal Stratification on MHD Oil Based Nanofluid

Ali Abdulsalam Abdulridha Als Salman, Abiodun Ezekiel Owoyemi, Ibrahim Mohammed Sulaiman*
Member, IAENG, Mustafa Mamat, Sunday Ezekiel Olowo

Abstract— This paper focuses on the thermal (ϵ_1) and solutal (ϵ_2) stratification on Magnetohydrodynamics (MHD) oil-based nanofluid. The local symmetry transformation is applied to convert the governing equations from partial differential equations (PDEs) into a set of non-Linear ordinary differential equations (ODEs). The fourth/fifth order Runge Kutta Fehlberg method with shooting scheme is applied for numerical simulation. Results obtained were plotted and analyzed. The Figures compared the reaction of both thermal stratification ($\epsilon_1 = 0.01, 0.9$) and solutal stratification ($\epsilon_2 = 0.01, 0.9$). The results show that there is significant positive correlation between them. It was gathered that the result of $\epsilon_1 = 0.01, \epsilon_2 = 0.01$ is higher when compare to $\epsilon_1 = 0.9, \epsilon_2 = 0.9$. Result indicates that thermal and solutal stratification temperature $\theta(\eta)$ and concentration $\phi(\eta)$ increase as a result of increase in the thermophores parameter, Nt , which is as result of the combine influences of the density and electric conductivity of the nanofluid.

Index Terms— MHD, nanofluid, solutal stratification, thermal stratification

I. INTRODUCTION

THE roles of thermal and solutal stratification on heat and mass transfer analysis in the boundary layer nanofluid flow over a stretching surface has key impact in industrial and engineering applications. For examples include, drawing on stretching sheets through quiescent fluids, compact heat exchangers, solar power collectors, manufacturing of plastic and rubber sheets, annealing and thinning of copper wires, boundary layer along a liquid film condensation process, damage of crops due to freezing, desalination, refrigeration and air conditioning, human transpiration and many others [1], [2].

One of the paramount disciplines for thermal engineering is heat transfer. There are three mechanisms in heat transfer

[3]. This includes conduction (in solid), convection (in liquid and gas) and radiation (through penetrating objects). In thermal convection, heat is being transferred via a mass movement of liquid (oil and gas), which is the main focus of this paper.

Therefore, it is paramount for researchers to explore more on the impacts of thermal conductivity that would supersede the traditional method. One of the mostly considered example of the traditional method is the theories of Maxwell [4]. The major drawback of the Maxwell's theories is that the cooling capacities is low [5], [6], [7]. Also, its behavior is insufficient when compared to the nanoparticle thermal conductivity.

Lately, several researches have been extensively done leading to the addition of based fluid [8]. In the late nineteenth century, Stephen U.S. Choi introduced a term called nanofluid [9]. This nanofluid comprises of a dispersal submicronic solid particle known as nanoparticle [10]. The main objective of the nanoparticle is to diffuse solid particle in fluid in order to boost thermal conductivity [11], [12], [13]. This approach has been further investigated and proved by several researchers [14] [15], [16], [17]. The nanoparticles can be obtained from metals such as *Al* and *Cu*, oxides such as Al_2O_3 and single surface carbon nanotubes (SWCNTs).

On the other hands, nanofluid can be described as a single stage composite of nanometer sized solid suspended particles and fibers in traditional base fluids. The frequently used based fluid are; oil, ethylene glycol mixture, toluene, etc. Nanofluids attempts many distinct assets in manufacturing employments such as; fuel cell, nuclear reactors, , transportation, microelectronics, and biomedicine [18], [19], [20] and [21].

Recently, several researchers have investigated the nanoparticles with the connection to industrial and engineering application. Some of such investigations cover area of oscillatory enhancement [22], nanoparticle effects on copper [23], stead and unsteady squeeze flow[4] and lots more. More so, these approaches have been applied to different area of chemical production [24], engineering [25], power development of a power plant [26], automotive [27], beforehand nuclear systems [28].

Result obtained in [29] considered the used of nanoparticles by avoiding overheat. [20] supported such and cited example of a computer system, where nanoparticles served as a coolant substance in heat transfers. The authors further explain that the presence of heat sink helps in

Manuscript received August 11, 2020; revised June 01, 2021.

Ali Abdulsalam Abdulridha Als Salman is currently a lecturer at the Department of Mathematics, University of Basrah College of Science, Basrah, Iraq (e-mail: aliafloong1988@gmail.com)

Abiodun Ezekiel Owoyemi is a researcher and acting head of department at the Department of General Studies, Federal College of Agricultural Produce Technology, Kano, Nigeria (e-mail: abiodunowoyemi9@gmail.com)

*Ibrahim Mohammed Sulaiman is a postdoctoral researcher at faculty of informatics and computing, Universiti Sultan Zainal Abidin, Malaysia (email: sulaimanib@unisza.edu.my)

Mustafa Mamat is a research Professor at University Malaysia Perlis, Perlis, Malaysia (must@unisza.edu.my)

Sunday Ezekiel Olowo is a research PhD student, and senior lecturer at the Department of Computer Science and Statistics, Federal College of Agricultural Produce Technology, Kano, Nigeria (e-mail: olowos@yahoo.com)

absorbing and cooling the heat generated from the system and thus, avoid being overheated. This is possible as a result of nanoparticle. Nanoparticle is ($< 100nm$) in diameter, which have impact in the liquid surface area properties. It has increase in the transfer of the heat when compare to micron-side particle [30].

[31] presented a paper on the two-non-dimensionless unsteady spill of a viscous MHD flow, which is in between two parallel infinite plate. The method of homotopy perturbation known as HPM has been used to obtain the velocity function for the parameter with a range of values. Furthermore, the effectiveness of HPM was demonstrated and the result obtained show that HPM has a significant advantage in the freedom of parameter selection.

The shape (sphere, cylinder and laminar) effects of the nanoparticle were recently investigated on squeeze MHD spill of water based above a penetrable sensor apparent for Cu, Al₂O₃ and SWCNTs as materials for transfer of heat. The result indicated that the sphere and cylinder shapes nanoparticle are more favorable in the shadow of Cu and SWCNTs in the performance of transfer heat boosting over a sensor apparent [32].

In this paper, our focus is to extend the work in [33], where the influence of governing parameters such as temperature, nanofluid volume fraction and fluid velocity were analyzed. In this present work, effort has been made to compare the reaction of both thermal stratification ($\epsilon_1 = 0.01, 0.9$) and solutal stratification ($\epsilon_2 = 0.01, 0.9$). The results show that there is significant positive correlation between them. Local symmetry transformation is adapted to convert the regulating PDEs into ODEs and then the numerical result of the problem is analyzed by utilizing Rung Kutta Fehlberg method of fourth or fifth order with shooting technique.

II. MATHEMATICAL ANALYSIS

In this paper, a steadier connective two-dimensional nanofluid flow with a solute thermal stratification is considered. Suppose x -axis is placed along the porous vertical plate and y -axis is assumed to be normal to the same plate. Let B_0 be activated in the positive direction of the x -axis. However, the ambient temperature along with the nanofluid concentration are considered to be $T_\infty = T_{\infty,0} + Ax$ and $C_\infty = C_{\infty,0} + Bx$, respectively, where the body surface is kept at a constant rate with T_w , and C_w being the nanofluid concentration. $T_{\infty,0}$ and $C_{\infty,0}$ is the depth of stratification. A and B remain constant values. The coordinate system and the flow structure is displaced in Fig. 1 [33]. Here, we follow

1) Continuity equation

$$\frac{\partial u}{\partial x} + \frac{\partial v}{\partial x} = 0 \tag{1}$$

2) Momentum equation

$$u \frac{\partial u}{\partial x} + v \frac{\partial u}{\partial y} = \nu \frac{\partial^2 u}{\partial y^2} - \left(\frac{\nu}{K} + \left(\frac{\sigma B_0^2}{\rho} \right) u \right) u \tag{2}$$

$$+(1 + C_{\infty,0})\rho f_{\infty,0}\beta g(T - T_{\infty,0}) - (\rho - \rho f_{\infty,0})g(T - T_{\infty,0})$$

3) Energy equation

$$u \frac{\partial T}{\partial x} + v \frac{\partial T}{\partial y} = \alpha \left(\frac{\partial^2 T}{\partial y^2} \right) + \tau \left\{ D_B \frac{\partial C}{\partial y} \frac{\partial T}{\partial y} + \frac{D_T}{T_\infty} \left(\frac{\partial T}{\partial y} \right)^2 \right\} \tag{3}$$

4) Diffusion equation

$$u \frac{\partial C}{\partial x} + v \frac{\partial C}{\partial y} = D_B \frac{\partial^2 C}{\partial y^2} + \frac{D_T}{T_\infty} \frac{\partial^2 T}{\partial y^2} \tag{4}$$

along with the boundary conditions

$$u = 0, v = -V_0, T = T_w, C = C_w, \text{ at } \eta = 0 \tag{5}$$

$$u = 0, T = T_\infty, C = C_\infty, \text{ and } \eta = \infty$$

Next, we have the local Rayleigh number along with the stream function ψ , respectively

$$Ra_x = \frac{(1+C_{\infty,0})\rho f_{\infty,0}\beta g(T-T_{\infty,0})}{\nu \alpha}, u = \frac{\partial \psi}{\partial y}, v = -\frac{\partial \psi}{\partial x} \tag{6}$$

Using the similarity transformation discussed below, we transform the energy equation, momentum equation, and diffusion equation into system of differential equation.

$$\eta = \frac{y}{x} Ra_x^{\frac{1}{4}}, \psi = Ra_x^{\frac{1}{4}} \alpha f(\eta),$$

$$\theta(\eta) = \frac{T - T_\infty}{T_w - T_{\infty,0}} - \frac{Ax}{T_w - T_{\infty,0}}, \tag{7}$$

$$\varphi(\eta) = \frac{C - C_\infty}{C_w - C_{\infty,0}} - \frac{Bx}{C_w - C_{\infty,0}}$$

where $C_w - C_{\infty,0} = mx, T_w - T_{\infty,0} = nx, m, n$ are constants.

- $Pr = \frac{\nu}{\alpha}$ - Prandtl number
- $Le = \frac{\nu}{D_B}$ - Lewis number
- $Nr = \frac{(\rho p + \rho f_{\infty,0})(C_w - C_{\infty,0})}{\rho f_{\infty,0} \beta (T_w - T_{\infty,0})(1 - C_{\infty,0})}$ - nanofluid buoyancy ratio,
- $Nb = \frac{(\rho c) \nu D_B (C_w - C_{\infty,0})}{(\rho c) \nu D_B (C_w - C_{\infty,0})}$ - nanofluid buoyancy ratio,
- $Nt = \frac{(\rho c) \nu D_T (T_w - T_{\infty,0})}{(\rho c) \nu D_T (T_w - T_{\infty,0})}$ - Brownian motion parameter
- $\epsilon_1 = \frac{4Ax}{(T_w - T_{\infty,0})} = \frac{4A}{n}$ - thermal stratification parameter,
- $\epsilon_2 = \frac{4Bx}{(C_w - C_{\infty,0})} = \frac{4A}{m}$ - solutal stratification parameter
- $\lambda = \frac{L^2}{K Ra_x^{1/2}}$ - porous parameter,
- $M = \frac{\sigma_0 B_0^2 L^2}{\mu Ra_x^{1/2}}$ - magnetic parameter,

However, the quantities parameters are;

- $C_f = \frac{\tau_w}{\rho_f U^2}$ - skin friction coefficient,
- $Nu_x = \frac{q_w x}{k_f (T_w - T_\infty)}$ - local Nusselt number,

where τ_w and q_w are defined as;

$$C_f (Re_\epsilon)^{\frac{1}{2}} = \frac{f''(0)}{(1-\gamma)^{2.5}}, \frac{Nu_x}{Re_\epsilon^{\frac{1}{2}}} = -\frac{K_{\tau_f}}{K_f} \theta'(0).$$

- $Re_\epsilon = \frac{U_x}{\nu_f}$ - The local Reynolds numbers.

After much algebraic works, we solved simultaneously, using 2-dimensional boundary layer for the four fundamental fluid dynamics equations, which are; energy equation, continuity equation, diffusion equation, and momentum equation. In this study, the flow of the system is steady.

$$u = hf'p,$$

$$\frac{\partial u}{\partial x} = -\frac{3}{4}\alpha \frac{Rax^{\frac{1}{2}}}{x} \eta f'' - \frac{1}{2}\alpha \frac{Rax^{1/2}}{x^2} f', \quad (8)$$

$$v = \frac{Rax^{\frac{1}{4}}}{x} \alpha \left[\frac{3\eta}{4} f' - \frac{1}{4} f \right].$$

$$\frac{\partial u}{\partial y} = hp^2 f'', \text{ and}$$

$$\frac{\partial^2 u}{\partial y^2} = hp^3 f''' \quad (9)$$

Along the x -axis and y -axis, we consider u and v as the velocity components respectively, while p and ρ are the pressure and density. The system of the equation is partially differential equations (PDEs) which are converted into the ODEs via similarity transformation. Furthermore, the PDE governing equation is converted into the following form of ODE. In the following section, we present the process of obtaining the ODEs from PDEs.

Momentum equation

Recall that; $u = hf'p$,

$$\frac{\partial u}{\partial x} = -\frac{3}{4}\alpha \frac{Rax^{\frac{1}{2}}}{x} \eta f'' - \frac{1}{2}\alpha \frac{Rax^{1/2}}{x^2} f',$$

$$v = \frac{Rax^{\frac{1}{4}}}{x} \alpha \left[\frac{3\eta}{4} f' - \frac{1}{4} f \right].$$

which follows that

$$\frac{\partial u}{\partial y} = hp^2 f''$$

and

$$\frac{\partial^2 u}{\partial y^2} = hp^3 f'''$$

Next is to show that the momentum equation is reduced to the following ODE.

$$u \frac{\partial u}{\partial x} + v \frac{\partial u}{\partial y} = v \frac{\partial^2 u}{\partial y^2} - \left(\frac{v}{K} + \frac{\sigma B_0^2}{\rho} \right) u + (1+C_{\infty,0}) \rho f_{\infty,0} \beta g (T-T_{\infty,0}) - (\rho - \rho f_{\infty,0}) g (T-T_{\infty,0})$$

$$hf'p \left[-\frac{3}{4}\alpha \frac{Rax^{\frac{1}{2}}}{x^2} \eta f'' - \frac{1}{2}\alpha \frac{Rax^{\frac{1}{2}}}{x^2} f' \right] + \frac{Rax^{\frac{1}{4}}}{x} \alpha \left[\frac{3\eta}{4} f' - \frac{1}{4} f \right] (hp^2 f'') =$$

$$vhp^3 f''' - \left(\frac{v}{K} + \frac{\sigma B_0^2}{\rho} \right) hf'p + (1+C_{\infty,0}) \rho f_{\infty,0} \beta g (T-T_{\infty,0}) - (\rho - \rho f_{\infty,0}) g (T-T_{\infty,0})$$

This implies

$$\frac{hf'p}{vhp^3} \left[-\frac{3}{4}\alpha \frac{Rax^{\frac{1}{2}}}{x} \eta f'' - \frac{1}{2}\alpha \frac{Rax^{\frac{1}{2}}}{x^2} f' \right] + \frac{hp^2 f''}{vhp^3} \frac{Rax^{\frac{1}{4}}}{x} \alpha \left[\frac{3\eta}{4} f' - \frac{1}{4} f \right] =$$

$$f''' - \frac{hf'p}{vhp^3} \left(\frac{v}{K} + \frac{\sigma B_0^2}{\rho} \right) + \frac{(1-C_{\infty,0}) \rho f_{\infty,0} \beta g (T-T_{\infty,0})}{vhp^3} - \frac{(\rho - \rho f_{\infty,0}) g (T-T_{\infty,0})}{vhp^3}$$

$$\frac{f'}{v \frac{(Ra_x)^{1/2}}{x^2}} \cdot \frac{(Ra_x)^{1/2}}{x^2} \left[-\frac{3}{4}\eta f'' - \frac{1}{2} f' \right]$$

The above expression can be simply obtained as follows

$$(1-C_{\infty,0}) \rho f_{\infty,0} \beta g (T-T_{\infty,0}) - (\rho - \rho f_{\infty,0}) g (T-T_{\infty,0})$$

Using the similarity transformation

$$\theta(\eta) = \frac{T - T_{\infty}}{T_w - T_{\infty,0}} - \frac{Ax}{T_w - T_{\infty,0}}$$

$$\varphi(\eta) = \frac{C - C_{\infty}}{C_w - C_{\infty,0}} - \frac{Bx}{C_w - C_{\infty,0}}$$

We have

$$\theta = \frac{T - T_{\infty}}{T_w - T_{\infty,0}} \Rightarrow T - T_{\infty,0} = \theta(T_w - T_{\infty,0}),$$

$$\varphi = \frac{C - C_{\infty}}{C_w - C_{\infty,0}} \Rightarrow C - C_{\infty,0} = (\varphi C_w - C_{\infty,0})$$

Substituting the value $T - T_{\infty,0} = \theta(T_w - T_{\infty,0})$ for $C - C_{\infty,0} = (\varphi C_w - C_{\infty,0})$

we obtain

$$\rho f_{\infty,0} (1 - C_{\infty,0}) \beta g [\theta(T_w - T_{\infty,0})] - (\rho - \rho f_{\infty,0}) g [(\varphi C_w - C_{\infty,0})]$$

and after some simplification become

$$\rho f_{\infty,0} (1 - C_{\infty,0}) (T_w - T_{\infty,0}) \beta g \left[\theta - \frac{(\rho - \rho f_{\infty,0}) g [(\varphi C_w - C_{\infty,0})]}{\rho f_{\infty,0} (1 - C_{\infty,0}) \beta g (T_w - T_{\infty,0})} \right]$$

$$\text{Also, recall here } Nr = \frac{(\rho p + \rho f_{\infty,0}) (C_w - C_{\infty,0})}{\rho f_{\infty,0} \beta (T_w - T_{\infty,0}) (1 - C_{\infty,0})}$$

is the nanofluid buoyancy ratio. Substituting this value will give

$$\frac{\rho f_{\infty,0} (1 - C_{\infty,0}) (T_w - T_{\infty,0}) \beta g [\theta - Nr \varphi]}{p^3 h v}$$

where

$$ph = \alpha \frac{Ra_x^{1/2}}{x} \text{ and } p^2 = \frac{Ra_x^{1/2}}{x}$$

And this becomes

$$\frac{\rho f_{\infty,0} (1 - C_{\infty,0}) (T_w - T_{\infty,0}) \beta g [\theta - N_r \varphi]}{\alpha \frac{Ra_x^{1/2}}{x} \left(\frac{Ra_x^{1/2}}{x} \right) \nu}$$

Also, recall that $R_{ax} = \frac{(1 - C_{\infty,0}) \beta g [\theta (T_w - T_{\infty,0})]}{\nu \alpha}$

$$\frac{\rho f_{\infty,0} (1 - C_{\infty,0}) (T_w - T_{\infty,0}) \beta g [\theta - N_r \varphi] x^2}{\alpha \nu \frac{(1 - C_{\infty,0}) (T_w - T_{\infty,0}) \beta g [\theta - N_r \varphi]}{\alpha \nu}}$$

By simplification, we obtain

$$\frac{1}{Pr} \left(-\frac{3}{4} \eta f f'' - \frac{1}{2} (f')^2 \right) + \frac{1}{Pr} \left(\frac{3}{4} \eta f' f'' - \frac{1}{4} f f''' \right) = f''' - f'(\lambda + M) + \rho f_{\infty,0} [\theta - N_r \varphi] x^2$$

which gives

$$\frac{1}{4Pr} (-2(f')^2 - f f''') = f''' - f'(\lambda + M) + [\theta - N_r \varphi] x^2$$

Therefore, employing the similarity transformation, the momentum equation, which is in the form of PDE is reduced to the following ODE;

$$f''' + \frac{3}{4Pr} (f f'' - (f')^2) + \theta - N_r \varphi - f'(\lambda + M) = 0 \quad (10)$$

Energy equation

Next, we also need to show how the energy equation is reduced to the ODE.

Recall that $u = hf'p$, and

$$\theta(\eta) = \frac{T - T_{\infty}}{T_w - T_{\infty,0}} - \frac{Ax}{T_w - T_{\infty,0}} \Rightarrow nx\theta(\eta) = T - T_{\infty,0}$$

So,

$$T = T_{\infty,0} + Ax + \theta nx$$

We then have

$$u \frac{\partial T}{\partial x} = hf'p \frac{\partial}{\partial x} (T_{\infty,0} + Ax + \theta nx)$$

Differentiating with respect to x , we have

$$u \frac{\partial T}{\partial x} = hf'p \left[A + \frac{\partial}{\partial x} (\theta nx) \right]$$

where,

$$\frac{\partial}{\partial x} (\theta nx) = n \frac{\partial}{\partial x} (\theta x) = n \left[\theta \frac{\partial}{\partial x} (x) + x \frac{\partial \theta}{\partial x} \right]$$

from

$$\frac{\partial}{\partial x} (\theta nx) = n \left[\theta + x \left(\frac{\partial \theta}{\partial \eta} \frac{\partial \eta}{\partial x} \right) \right]$$

and $\eta = \frac{y}{x^2} Ra_x^{\frac{3}{4}}$

By substituting, we get

$$\frac{\partial}{\partial x} (\theta nx) = n \left[\theta + x \left(\frac{\partial \theta}{\partial \eta} \frac{\partial \left(\frac{y}{x} Ra_x^{\frac{3}{4}} \right)}{\partial x} \right) \right]$$

Differentiating the above equation, we obtain

$$\frac{\partial}{\partial x} (\theta nx) = n \left[\theta + \left(\theta' \cdot \frac{3}{4} \left(\frac{y}{x} Ra_x^{\frac{3}{4}} \right) \right) \right]$$

and factorising gives

$$\frac{\partial}{\partial x} (\theta nx) = n\theta - \frac{3}{4} \theta' ny \left(\frac{Ra_x^{\frac{1}{4}}}{x} \right)$$

Also, after substitution, we have

$$u \frac{\partial T}{\partial x} = hf'p \left[A + n\theta - \frac{3}{4} \theta' ny \left(\frac{Ra_x^{\frac{1}{4}}}{x} \right) \right]$$

Given

$$v = \frac{3}{4} yf' \alpha \frac{Ra_x^{\frac{1}{4}}}{x} - \frac{1}{4} f \alpha \frac{Ra_x^{\frac{1}{4}}}{x}$$

$$v \frac{\partial T}{\partial y} = \left[\frac{3}{4} yf' \alpha \frac{Ra_x^{\frac{1}{4}}}{x} - \frac{1}{4} f \alpha \frac{Ra_x^{\frac{1}{4}}}{x} \right] \frac{\partial T}{\partial y}$$

Thus, by substitution and applying the chain rule, we obtain

$$\frac{\partial T}{\partial y} = \frac{\partial}{\partial y} (\theta nx) = nx \frac{\partial}{\partial y} (\theta) = nx \frac{\partial \theta}{\partial \eta} \frac{\partial \eta}{\partial y}$$

and

$$\eta = \frac{y}{x} Ra_x^{\frac{3}{4}} \Rightarrow \frac{\partial \eta}{\partial y} = \frac{Ra_x^{\frac{3}{4}}}{x}$$

Hence,

$$\frac{\partial T}{\partial y} = n\theta' Ra_x^{\frac{1}{4}}$$

which implies that

$$\frac{\partial T}{\partial y} = \left[\frac{3}{4} yf' \alpha \frac{Ra_x^{\frac{1}{4}}}{x} - \frac{1}{4} f \alpha \frac{Ra_x^{\frac{1}{4}}}{x} \right] n\theta' Ra_x^{\frac{1}{4}}$$

But given that

$$\varphi(\eta) = \frac{C - C_{\infty}}{C_w - C_{\infty,0}} - \frac{Bx}{C_w - C_{\infty,0}} \Rightarrow \varphi mx = c - C_{\infty,0} - Bx$$

Then,

$$c = C_{\infty,0} + Bx + \varphi mx,$$

and

$$\frac{\partial C}{\partial y} = mx \left(\frac{\partial \phi}{\partial \eta} \frac{\partial \eta}{\partial y} \right).$$

Hence,

$$\frac{\partial C}{\partial y} = mRa_x^{\frac{1}{4}} \phi'$$

which gives

$$hf'p \left[A + n\theta - \frac{3}{4} \theta' ny \left(\frac{Ra_x^{\frac{1}{4}}}{x} \right) \right] + \left[\frac{3}{4} yf' \alpha \frac{Ra_x^{\frac{1}{4}}}{x} - \frac{1}{4} f \alpha \frac{Ra_x^{\frac{1}{4}}}{x} \right] n\theta' Ra_x^{\frac{1}{4}} = \alpha \frac{n}{x} Ra_x^{\frac{1}{2}} \theta'' +$$

$$\tau \left\{ D_B \left(mRa_x^{\frac{1}{4}} \phi' \right) \left(n\theta' Ra_x^{\frac{1}{4}} \right) + \frac{D_T}{T_\infty} n^2 Ra_x^{\frac{1}{2}} (\theta')^2 \right\}$$

$$\frac{1}{\alpha \frac{n}{x} Ra_x^{\frac{1}{2}}} \left[hf'p \left[A + n\theta - \frac{3}{4} \theta' ny \left(\frac{Ra_x^{\frac{1}{4}}}{x} \right) \right] + \left[\frac{3}{4} yf' \alpha \frac{Ra_x^{\frac{1}{4}}}{x} - \frac{1}{4} f \alpha \frac{Ra_x^{\frac{1}{4}}}{x} \right] n\theta' Ra_x^{\frac{1}{4}} \right] =$$

$$\alpha \frac{n}{x} Ra_x^{\frac{1}{2}} \theta'' + \tau \left\{ D_B \left(mRa_x^{\frac{1}{4}} \phi' \right) \left(n\theta' Ra_x^{\frac{1}{4}} \right) + \frac{D_T}{T_\infty} n^2 Ra_x^{\frac{1}{2}} (\theta')^2 \right\}$$

$$\frac{1}{\alpha \frac{n}{x} Ra_x^{\frac{1}{2}}} \left[hf'p \left[A + n\theta - \frac{3}{4} \theta' ny \left(\frac{Ra_x^{\frac{1}{4}}}{x} \right) \right] \right]$$

where $p = \frac{Ra_x^{\frac{1}{2}}}{x}$ and $ph = \alpha \frac{Ra_x^{\frac{1}{2}}}{x}$.

Now, we simplify to get

$$\frac{Af'}{n} + f'\theta - \frac{3}{4} f'\theta y \left(\frac{Ra_x^{\frac{1}{4}}}{x} \right)$$

and

$$\frac{3}{4} f'\theta y \left(\frac{Ra_x^{\frac{1}{4}}}{x} \right)$$

Factorising the above will lead to

$$\theta'' - f'\theta + \frac{1}{4} f'\theta - \frac{\varepsilon_1 f'}{n} + Nb\phi'\theta' + Nt(\theta')^2 = 0 \quad (11)$$

where

$$\varepsilon_1 = \frac{4A}{\eta} \Rightarrow \frac{A}{\eta} = \frac{\varepsilon_1}{\eta}$$

Eq. (11) is the solution of energy equation from PDE into ODE

Diffusion equation

In this subsection, we reduce our given diffusion equation into the ODE. In this case, we shall solve each part separately as usual

where $u = hf'p$ and

$$\frac{\partial C}{\partial x} = B + m\phi - \frac{3}{4} m\phi' y \frac{Ra_x^{\frac{1}{4}}}{x}$$

Considering the first part, we have

$$hf'p \left(B + m\phi - \frac{3}{4} m\phi' y \frac{Ra_x^{\frac{1}{4}}}{x} \right)$$

$$v = \frac{3}{4} f'y \alpha \frac{Ra_x^{\frac{1}{2}}}{x^2} - \frac{1}{4} f \alpha \frac{Ra_x^{\frac{1}{4}}}{x}$$

and

$$\frac{\partial C}{\partial y} = mRa_x^{\frac{1}{4}} \phi'$$

$$\left(\frac{3}{4} f'y \alpha \frac{Ra_x^{\frac{1}{2}}}{x^2} - \frac{1}{4} f \alpha \frac{Ra_x^{\frac{1}{4}}}{x} \right) \left(mRa_x^{\frac{1}{4}} \phi' \right)$$

and

$$\frac{\partial^2 T}{\partial y^2} = \frac{n}{x} \theta'' Ra_x^{\frac{1}{4}}$$

Solving the above equation will give

$$hf'p \left(B + m\phi - \frac{3}{4} mRa_x^{\frac{1}{4}} \phi' \right) + \left(\frac{3}{4} f'y \alpha \frac{Ra_x^{\frac{1}{2}}}{x^2} - \frac{1}{4} f \alpha \frac{Ra_x^{\frac{1}{4}}}{x} \right) \left(mRa_x^{\frac{1}{4}} \phi' \right) =$$

$$D_B \left(m\phi'' \frac{Ra_x^{\frac{1}{2}}}{x} \right) + \frac{D_T}{T_\infty} \frac{n}{x} \theta'' Ra_x^{\frac{1}{4}}$$

After simplification, it becomes

$$\frac{\alpha f'B}{D_B m} + \frac{\alpha f'\phi}{D_B} - \frac{3}{4} \frac{\alpha y \phi' m Ra_x^{\frac{1}{4}}}{D_B x} + \frac{\frac{3}{4} \alpha f'\phi' y Ra_x^{\frac{1}{4}}}{D_B x} - \frac{\frac{1}{4} \alpha f \phi'}{D_B} = \phi'' + \frac{D_T}{T_\infty} \frac{n}{D_B} \theta''$$

which is reduced to

$$\phi'' - Le\phi' + \frac{1}{4} Le\phi' - Le\phi' \frac{\varepsilon_2}{4} + \frac{\alpha f'\theta''}{Nb} = 0 \quad (12)$$

where

$$\varepsilon_2 = \frac{4B}{m} \Rightarrow \frac{B}{m} = \frac{\varepsilon_2}{4} \text{ and } Le = \frac{\alpha}{D_B}$$

Therefore, eq. (12) gives the solution of diffusion equation into ODE

III. NUMERICAL TECHNIQUE

The solved energy, momentum, and diffusion equations are transformed from its third-order equation to the first-

order equation, and then, from second-order equation to the first-order equation respectively, as given in (13-15),

$$\begin{cases} f(\eta) = f(\eta) \\ f'(\eta) = u(\eta) \\ f''(\eta) = u'(\eta) = v(\eta) \\ f'''(\eta) = u''(\eta) = v'(\eta) \end{cases} \quad (13)$$

$$\begin{cases} \theta(\eta) = \theta(\eta) \\ \theta'(\eta) = w(\eta) \\ \theta''(\eta) = w'(\eta) \end{cases} \quad (14)$$

$$\begin{cases} \varphi(\eta) = \theta(\eta) \\ \varphi'(\eta) = w(\eta) \\ \varphi''(\eta) = w'(\eta) \end{cases} \quad (15)$$

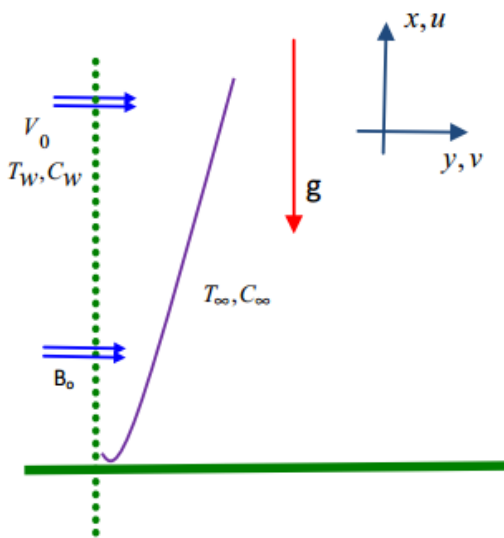


Fig 1: Flow structure and coordinate system

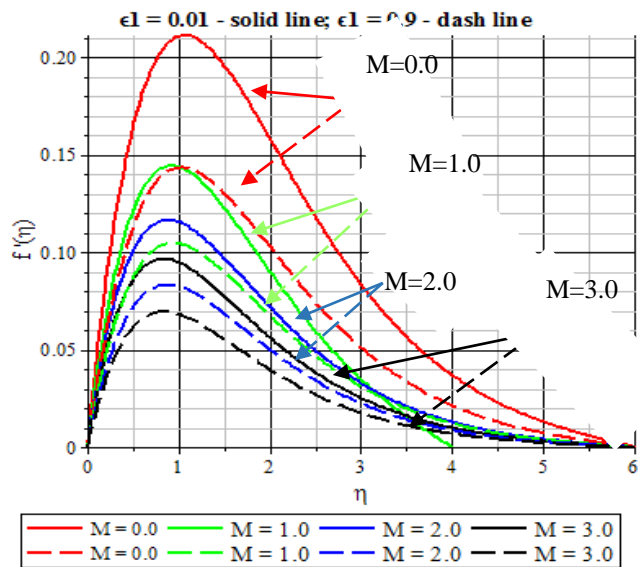
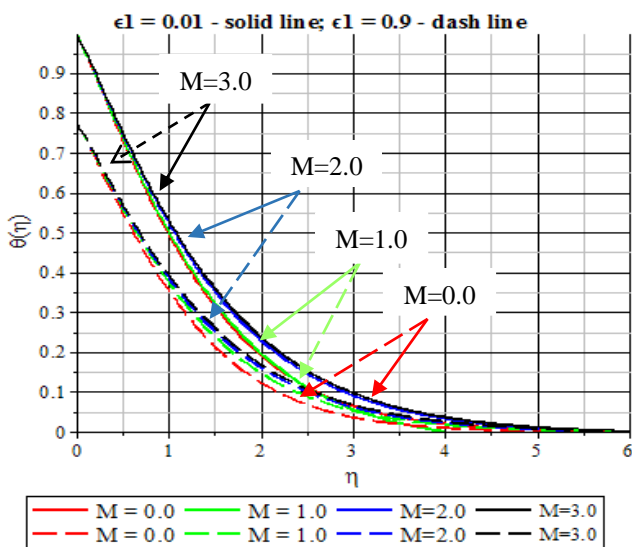


Fig 2: Comparison of the magnetic effects profile of velocity, temperature, and concentration of current work with Fig, 9 in [33]

IV. RESULTS AND DISCUSSION

In this section, the numerical simulation is illustrated and discussed. The result was analyzed with certain nanofluid flows. The Runge Kutta Fehlberg technique of fourth/fifth order was applied together with the shooting method. The software used in the analysis was Maple 18 platform. Three Figures are displayed for each including and concentration $\varphi(\eta)$, temperature $\theta(\eta)$, and velocity $f(\eta)$. The effect that involves in the magnetic field, radiation, heat source, heat sink, suction, injection, porous and volume fraction is being analyzed at each section.

The parameters ($M, \lambda, S, Nr, Nb, Nt$) are numerically executed for governing equations (ODEs) along with boundary conditions in equation. In this regard, the shooting technique is employed to solved the ODEs along with the conditions. This shooting technique was introduced by Runge Kutta in the nineteen century and has been recently studied by many researchers [34]–[36].

We set the parameter to use. The analysis reports the parameters' effects on the thermal and solutal stratification on MHD oil based nanofluid (Crude oil, $Pr = 1490.51$). The parameters and its value include:

1. Magnetic field, M : 0.0, 1.0, 2.0, 3.0.
2. Thermal porous, λ : 0.0, 0.5, 1.0, 3.0.
3. Buoyancy, Nr : 0.0, 0.3, 0.6, 0.8.
4. Brownian motion, Nb : 0.1, 0.3, 0.5, 0.9.
5. Suction, $S > 0$: 0.0, 0.5, 1.0, 2.0.
6. Thermophoresis, Nt : 0.0, 0.2, 0.5, 0.8.

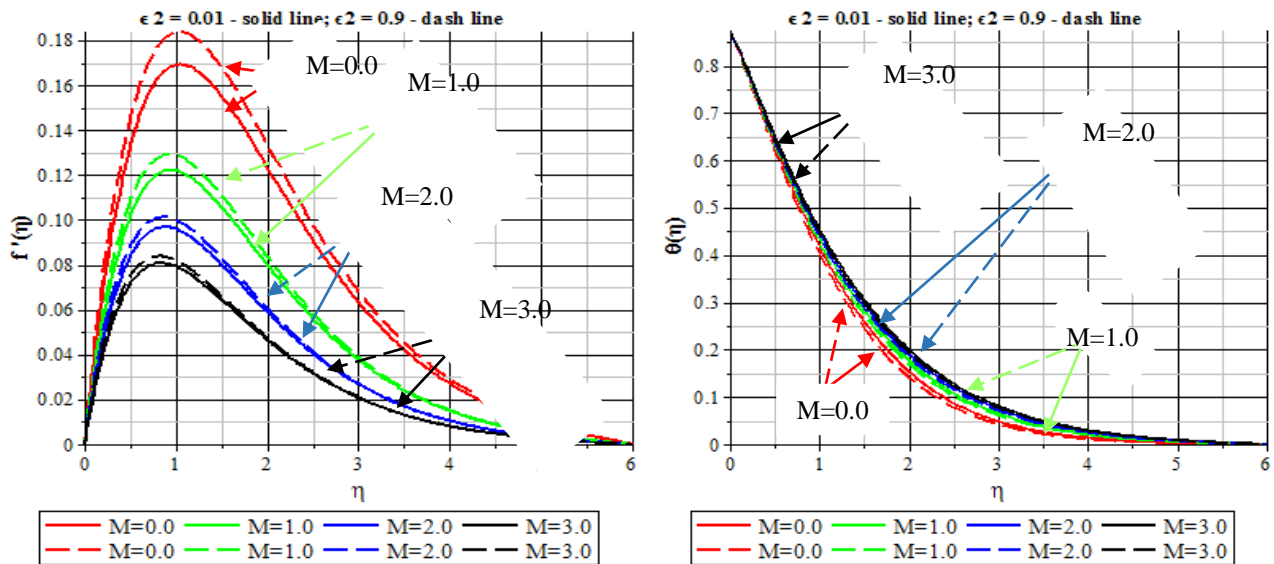


Fig 3 Comparison of magnetic strength on velocity and temperature profiles with Fig, 6 in [33]

In order to validate our results, Fig, 2-3. display the comparison result of the thermal (ϵ_1) and solutal (ϵ_2) stratification on magnetic effects profile for both the velocity and the temperature. The obtained results are in excellent agreement with those obtained in [33].

TABLE 1. The rate of skin friction, rate of heat transfers and transfer of mass with the impact of Magnetic Field M, based upon thermal and solutal stratification boundary

M	$f''(0)$	$-\theta'(0)$	$-\phi'(0)$	Remark
0.0	0.466315	0.468629	3.396999	$\epsilon_1 = 0.01$
1.0	0.375512	0.454320	3.330739	
2.0	0.323670	0.446329	3.296400	
3.0	0.288670	0.441046	3.274743	
0.0	0.371685	0.431175	3.465930	$\epsilon_2 = 0.9$
1.0	0.303292	0.413191	3.448117	
2.0	0.262400	0.403268	3.437767	
3.0	0.234258	0.396843	3.430857	

Table 1. above indicates that when magnetic field, M , is increasing, the skin friction is reducing. The value for the concentration, $-\phi'(0)$ is considered quite low when compared to the temperature. In the case of solutal stratification parameter $\epsilon_2 = 0.09$, temperature, $-\theta'(0)$ and concentration $-\phi'(0)$ reduce as the magnetic field increases.

TABLE 2. The rate of skin friction, rate of heat transfers and transfer of mass with the impact of Brownian motion Nb , based upon thermal and solutal stratification boundary

M	$f''(0)$	$-\theta'(0)$	$-\phi'(0)$	Remark
0.1	0.254288	0.606220	0.908983	$\epsilon_1 = 0.01$
0.3	0.351042	0.531251	2.939696	
0.5	0.375512	0.454320	3.330739	
0.8	0.399739	0.328111	3.575632	
0.1	0.223049	0.561986	0.526862	
0.3	0.312361	0.509835	2.481040	

0.5	0.334367	0.447280	2.868760	$\epsilon_2 = 0.9$
0.8	0.355274	0.339364	3.120368	

In Table 2., the result displayed that thermal stratification parameter at $\epsilon_1 = 0.01$, when Brownian motion. Nb , is increasing, the skin friction $f''(0)$, is also increasing. the rate of heat transfer, $-\theta'(0)$ is increasing also. Moreover, the Brownian motion. Nb increase as a result of increase in the concentration, $-\phi'(0)$. The movement of the nanoparticle is associated with the concentration, $-\phi'(0)$.

TABLE 3. The rate of skin friction, rate of heat transfers and transfer of mass with the impact of Buoyancy Nr , based upon thermal and solutal stratification boundary

M	$f''(0)$	$-\theta'(0)$	$-\phi'(0)$	Remark
0.0	0.4830015	0.459488	3.350874	$\epsilon_1 = 0.01$
0.3	0.418704	0.456422	3.338936	
0.6	0.353817	0.453251	3.326564	
0.9	0.327822	0.300080	3.592864	
0.0	0.413510	0.451165	2.891033	$\epsilon_2 = 0.9$
0.3	0.366230	0.448868	2.877904	
0.6	0.318324	0.444646	2.864060	
0.9	0.269724	0.443952	2.849395	

Table 3. indicates that when Buoyancy, Nr , increase as a result of decrease in the skin friction, $f''(0)$, is decreasing, while, the heat transfer rate, $-\theta'(0)$ barely increase. Also, as the Buoyancy, Nr increase, the concentration, $-\phi'(0)$ are increase. There is increase in value for the thermal stratification, which indicated that the heat transfers mostly from the surface to the fluid.

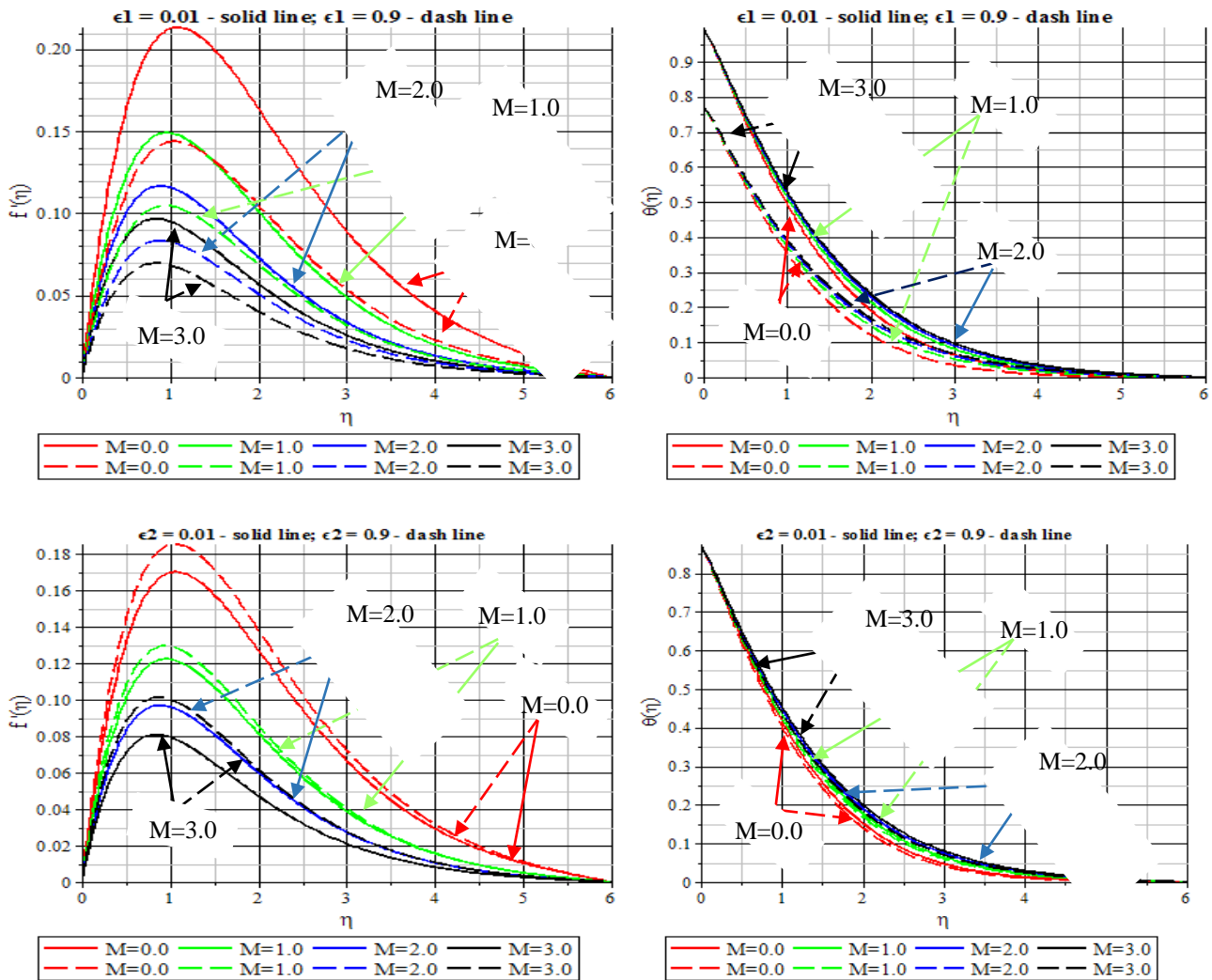
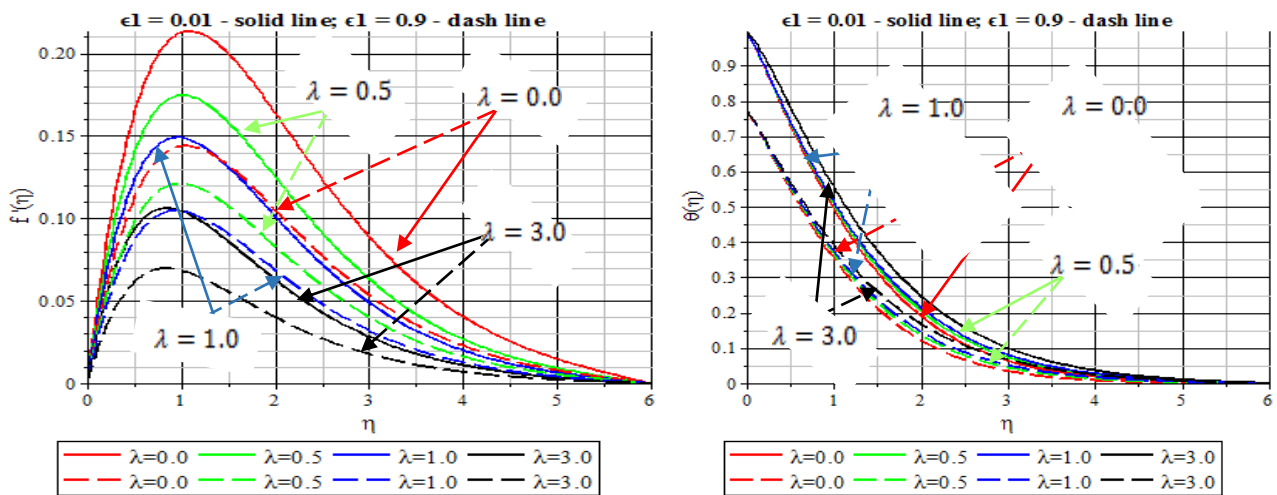


Fig 4: Magnetic field M , on velocity $f(\eta)$, and temperature $\theta(\eta)$ profiles

For the thermal stratification (ϵ_1), the velocity $f(\eta)$, increase with decrease in the magnetic strength. The temperature increases as result of increase in the magnetic straight. Whereas, for the solutal stratification. ϵ_2 , the nanofluids velocity decrease as a result of increase in the magnetic strength. The temperature, $\theta(\eta)$, of heat transfer

rate $\varphi(\eta)$, increase with increase in thermal magnetic power for solutal, which is due to the Lorentz force falls down the motion of the fluid and to enhance the temperature profiles. the result of $\epsilon_1 = 0.01, \epsilon_2 = 0.01$ is higher when compare to $\epsilon_1 = 0.9, \epsilon_2 = 0.9$.



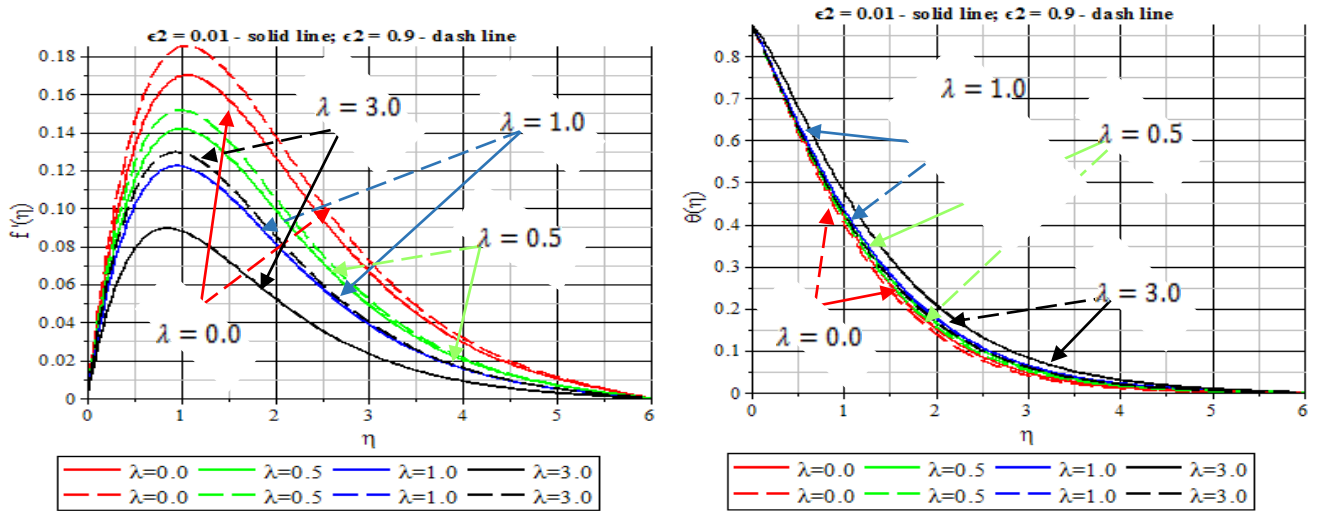


Fig 5: porous, λ on velocity $f(\eta)$, and temperature $\theta(\eta)$ profiles

Figure5: Discussion of porous parameter λ .

Both thermal stratification (ϵ_1), and stratification (ϵ_2), velocity $f(\eta)$, increase as a result of decrease in the porous parameter, λ . Whereas the temperature increases as result of increase in the porous parameters. This is because of the

Lorentz force falls down the motion of the fluid and as a result it boosts the temperature profiles. This is due to the mixed effect of permeability of the porous medium and the kinematic viscosity of the nanofluid.

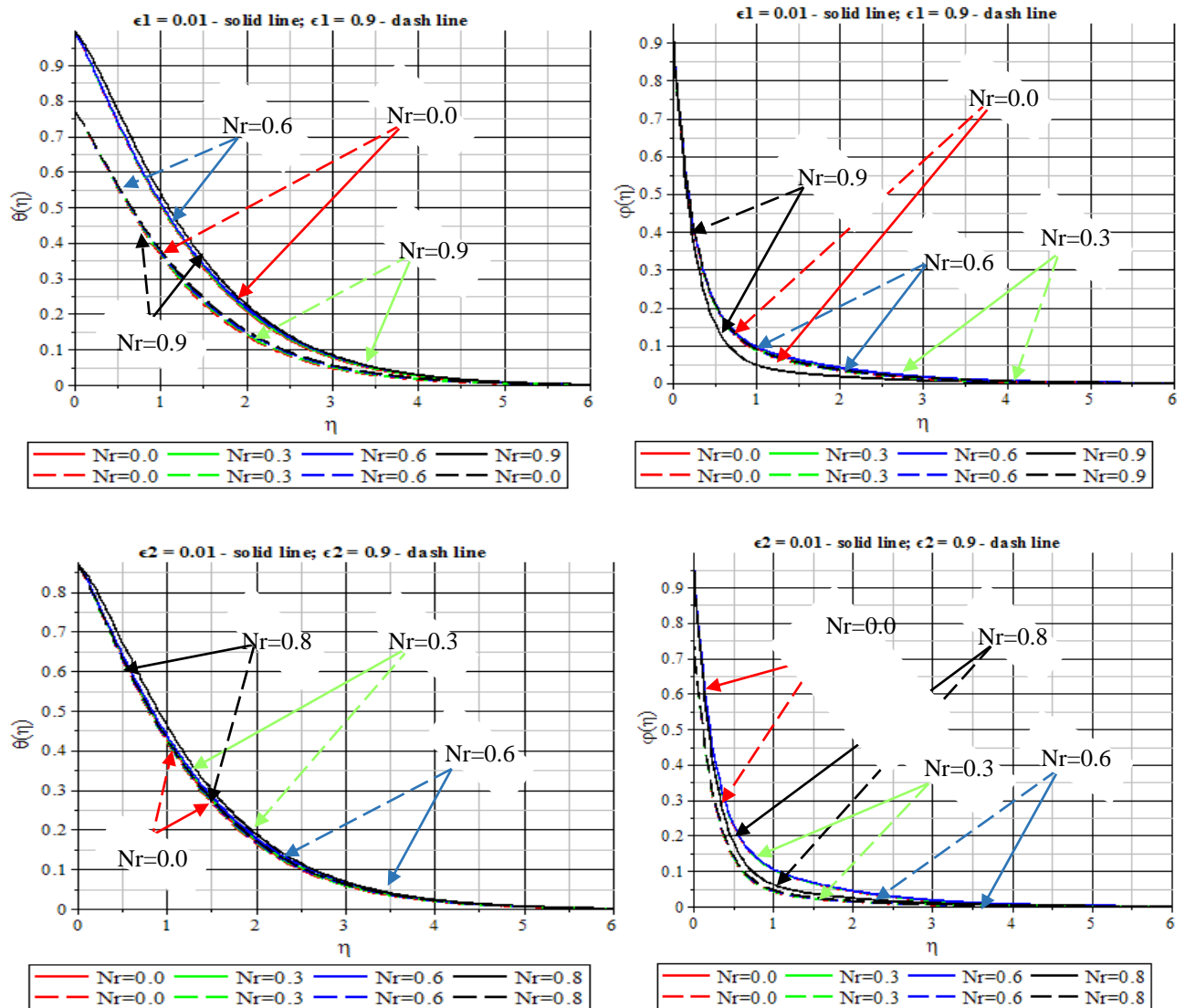
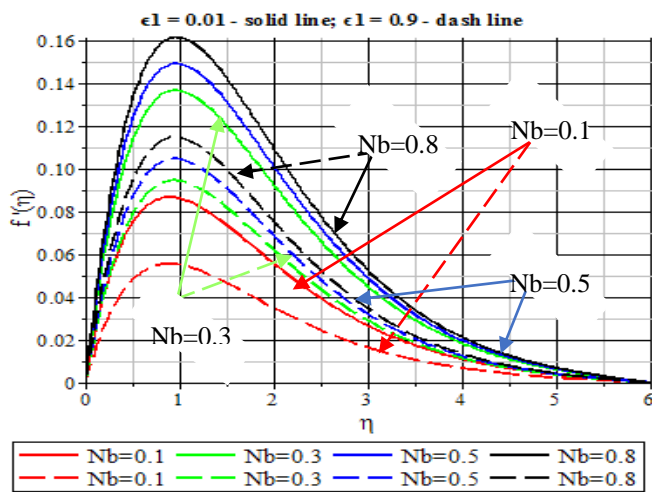


Fig 6: Buoyancy, Nr , on temperature, $\theta(\eta)$, and concentration, $\phi(\eta)$ profiles

Figure 6: Discussion buoyancy parameter, Nr .

Fig,4 indicated that the thermal stratification at $\epsilon_2 = 0.01$ is higher than when it is fixed at $\epsilon_2 = 0.09$. Both the on temperature, $\theta(\eta)$, and concentration, $\varphi(\eta)$ profiles increase



buoyancy parameter, Nr increase with a major significant. This is as obtained as a result of join influence of the nanoparticle mass density and thermal coefficient reaction of the crude oil-based fluid with the Lorentz force, which play a dominant role on the nanofluid flow field.

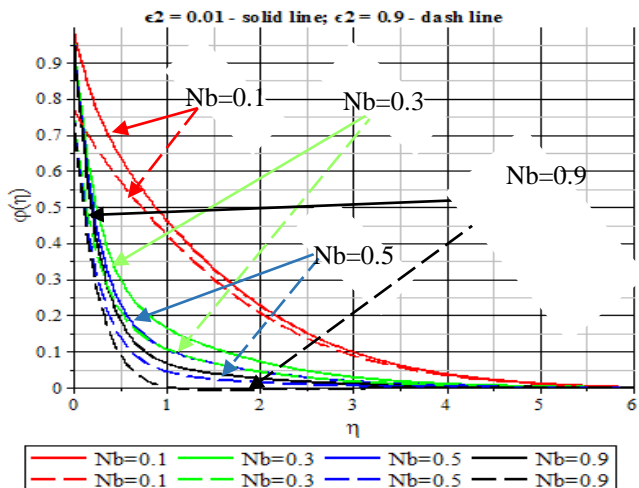
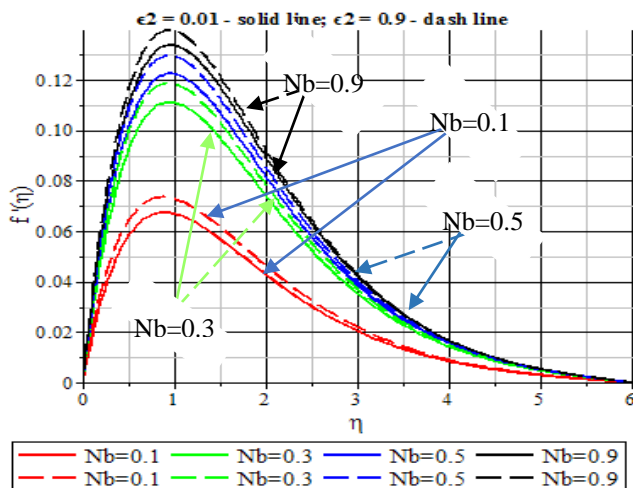
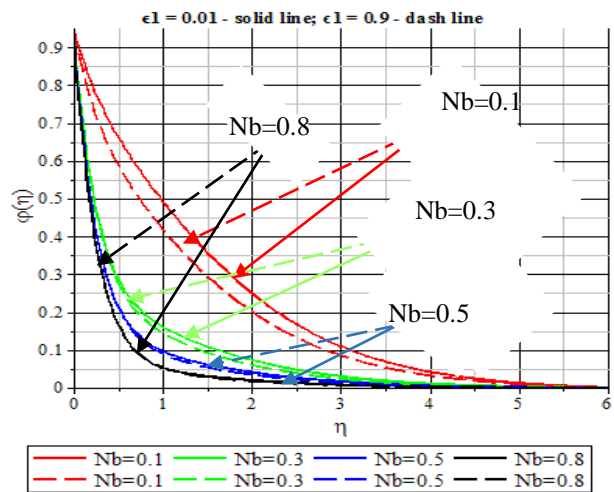


Fig 7: Brownian motion, Nb , on velocity, $f'(\eta)$, and concentration, $\varphi(\eta)$ profiles

Figure 7: Discussion of Brownian motion parameter Nb .

It shows the Figure of $f(\eta)$, and $\varphi(\eta)$ circulation in the presence of solutal and thermal stratification $\epsilon = 0.01, 0.09$.

Both thermal and solutal stratification velocity $f(\eta)$, increase as a result of the increase in the Brownian motion. Also, it indicated temperature decreased which subsequently increased the temperature when the Brownian motion is increasing. This is due to movement rate of nanoparticles which is associated with the viscosity and concentration of the nanofluid.

Table 4. Effects of the thermophores, Nt , on solutal and thermal stratification parameter in the presence of heat

Nt	$-\theta'(\eta)$ at ϵ_1	$-\theta'(\eta)$ at ϵ_2
0.0	0.556255	0.493900
0.2	0.512135	0.459223
0.5	0.454320	0.413191
0.8	0.269487	0.246228

Table 5. Effects of the thermophores, Nt , on thermal and solutal stratification parameter in the presence of mass transfer

Nt	$-\varphi'(\eta)$ at ϵ_1	$-\varphi'(\eta)$ at ϵ_2
0.0	3.692660	3.794515
0.2	3.524618	3.637558
0.5	3.330739	3.448117
0.8	3.579769	3.662381

Tables 4-5 displays the reaction of thermophoresis, Nt , the reaction indicated that the increase in thermophores effect the increase in both the bottom layer and higher layer, the temperature will increase and the concentration increasing also. The thermal stratification parameter layer shows more significant effect on the thermophores than the solutal stratification parameter.

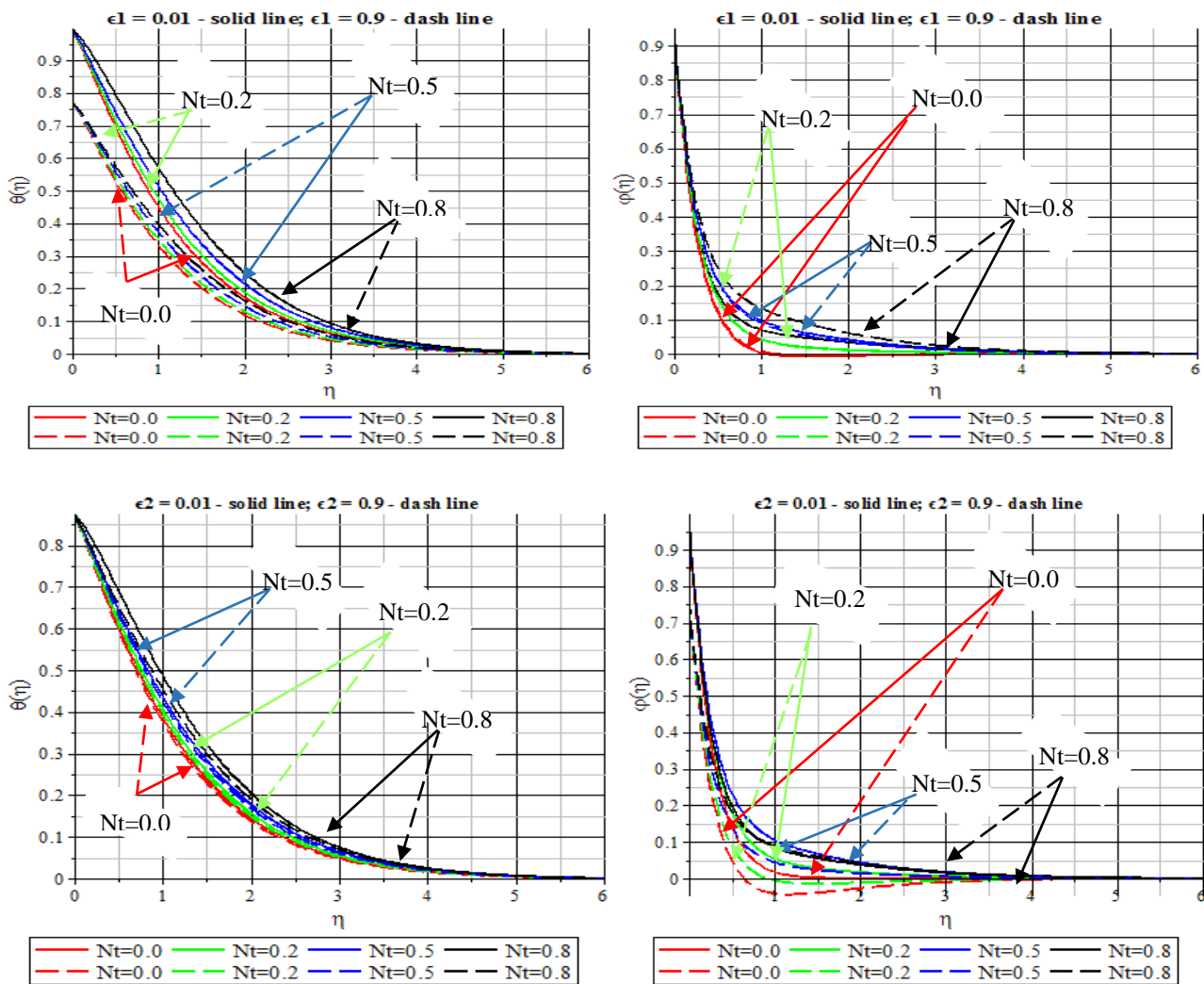


Fig 8: Thermophores, Nt , on temperature, $\theta(\eta)$ and concentration, $\varphi(\eta)$ for ϵ_1 and ϵ_2 profiles

Figure 8: Discussion of thermophores parameter Nt . Both the temperature $\theta(\eta)$ and concentration $\varphi(\eta)$ increase as a result of increase in the thermophores parameter, Nt circulation in the presence of both thermal stratification $\epsilon_1 = 0.01, 0.9$ and solutal stratification $\epsilon_2 = 0.01, 0.9$. Also, it indicated that the thermophores parameters $Nt = 0.0, 1.0, 2.0, 3.0$ effect with high electric field, as result of the combine influence of the density and electric conductivity of the nanofluid. This implies that the thermophore is dominate on the transfer of heat.

Table 6. Effects of the Suction/injection, S , on solutal and thermal stratification parameter in the presence of heat

S	$-\theta'(\eta)$ at ϵ_1	$-\theta'(\eta)$ at ϵ_2
0.0	-0.159999	-0.63395
0.5	-0.290917	-1.883656
1.0	-0.454320	-3.330739
2.0	-0.832201	-6.381059

Table 7. Effects of the Suction/injection, S , on solutal and thermal stratification parameter in the presence of mass transfer

S	$-\varphi'(\eta)$ at ϵ_1	$-\varphi'(\eta)$ at ϵ_2
0.0	-0.156539	-0.502096
0.5	-0.272142	-1.853734
1.0	-0.413191	-3.448118
2.0	-0.740355	-6.780016

Tables 6-7 displays the reaction of Suction/injection, S . The tables give the different values of magnetic strength in the presence of injection $S = 0.0, 0.5, 1.0, 2.0$ and with uniform Prandtl number $Pr = 1490.51$. Due to the injection with uniform Prandtl number $Pr = 1490.51$, both the temperature and concentration of the nanofluid firstly decreases as a result of decrease in the Suction parameters. Lorentz force low down the movement of the fluid and to increase the temperature profiles.

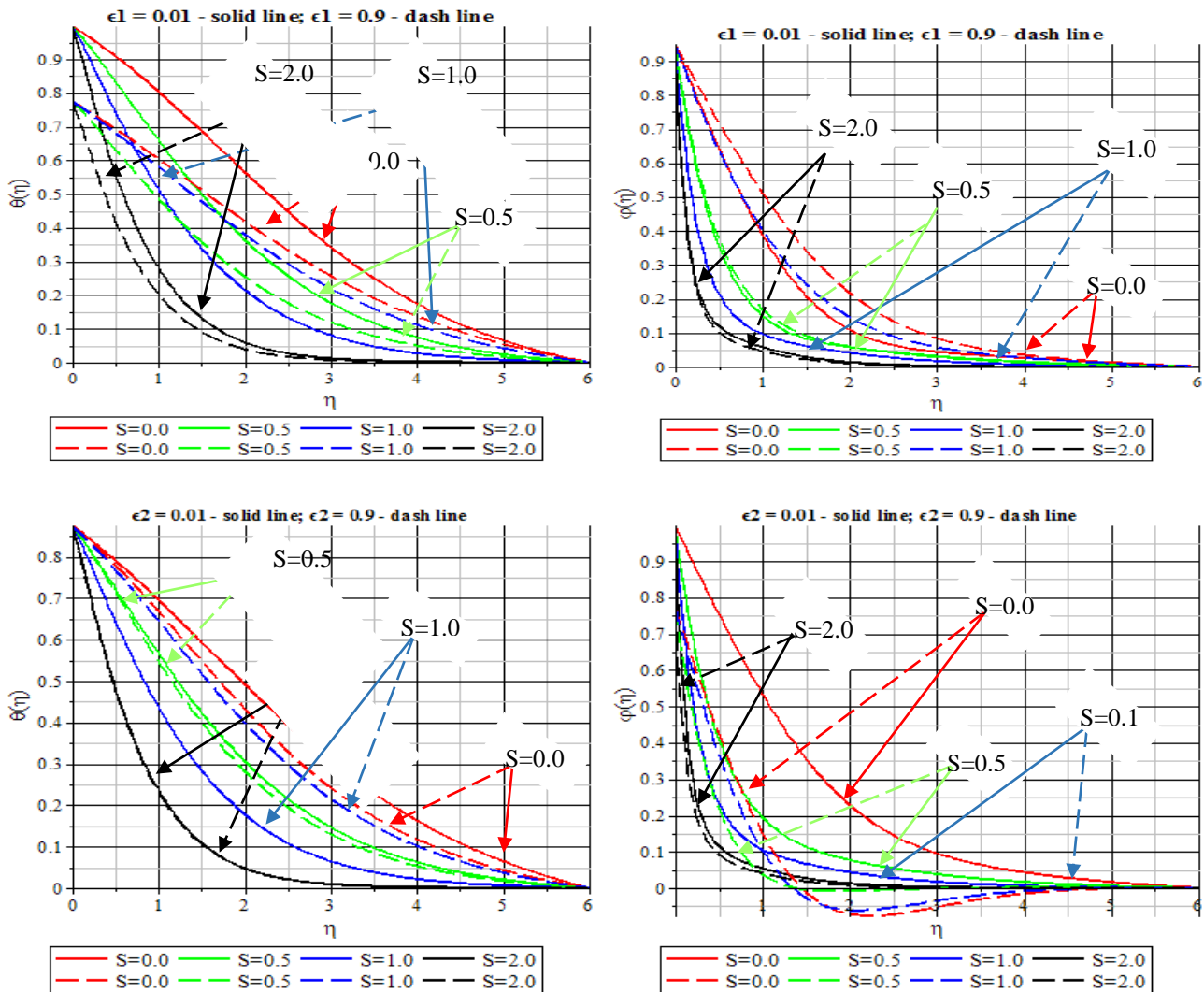


Fig 9: Suction/injection, S , on temperature, $\theta(\eta)$ and concentration, $\varphi(\eta)$ for ϵ_1 and ϵ_2 profiles

Fig 9, discussion of thermophores parameter, Nt

The figure presents the temperature and concentration for different values of magnetic strength in the presence of injection $S = 0.0, 0.5, 1.0, 2.0$ and with uniform Prandtl number $Pr = 1490.51$. Due to the injection with uniform Prandtl number $Pr = 1490.51$, both the temperature and concentration of the nanofluid firstly decreases as a result of decrease in the Suction parameters. Lorentz force low down the movement of the fluid and to increase the temperature profiles.

V. RESULTS AND DISCUSSION

The paper presented the thermal (ϵ_1) and solutal (ϵ_2) stratification on Magnetohydrodynamics (MHD) oil-based nanofluid. The local symmetry transformation is applied to convert the governing equations from PDEs into a set of

non-Linear ordinary differential equations ODEs. The fourth/fifth order Runge Kutta Fehlberg method with shooting scheme was applied for numerical simulation. Results obtained were plotted and analyzed. The Figures compared the reaction of both thermal stratification ($\epsilon_1 = 0.01, 0.9$) and solutal stratification ($\epsilon_2 = 0.01, 0.9$).

The results show that there is significant positive correlation between them.

Various variable of the parameters were handled and manipulated as the constant variable. Some of the reactions are given as follows:

1. The result of $\epsilon_1 = 0.01, \epsilon_2 = 0.01$ is higher when compare to $\epsilon_1 = 0.9, \epsilon_2 = 0.9$.
2. The thermal and solutal stratification temperature $\theta(\eta)$ and concentration $\varphi(\eta)$ increase as a result of increase in the thermophores parameter, Nt , which is as result of the combine influences of the density. and electric conductivity of the nanofluid.
3. Both the temperature $\theta(\eta)$ and concentration $\varphi(\eta)$ increase as a result of increase in the thermophores parameter, Nt parameters
4. It indicated temperature decreased which subsequently increased the temperature when the Brownian motion is increasing. This is as a result of the rate of movement of nanoparticles, which is associated with the viscosity and concentration of the nanofluid.
5. It shows the Fig. of velocity $f(\eta)$, and temperature $\theta(\eta)$ circulation in the presence of solutal and

thermal stratification. $\epsilon_1 = 0.01, 0.9$ and $\epsilon_2 = 0.01, 0.09$ respectively.

6. It also indicates that different values of magnetic strength in the presence of injection $S = 0.0, 0.5, 1.0, 2.0$ and with uniform Prandtl number $Pr = 1490.51$.

ACKNOWLEDGMENT

Ibrahim Mohammed Sulaiman would like to thank the Postdoctoral Fellowship from Universiti Sultan Zainal Abidin, Terengganu, Malaysia.

REFERENCES

- [1] T. Hayat, T. Muhammad, S. A. Shehzad, and A. Alsaedi, "An analytical solution for magnetohydrodynamic Oldroyd-B nanofluid flow induced by a stretching sheet with heat generation/absorption," *Int. J. Therm. Sci.*, vol. 111, pp. 274–288, 2017.
- [2] T. Hayat, S. Ali Shehzad, M. Mustafa, and A. Hendi, "MHD flow of an oldroyd-B fluid through a porous channel," *Int. J. Chem. React. Eng.*, vol. 10, no. 1, 2012.
- [3] P. Keblinski, S. R. Phillpot, S. U. S. Choi, and J. A. Eastman, "Mechanisms of heat flow in suspensions of nano-sized particles (nanofluids)," *Int. J. Heat Mass Transf.*, vol. 45, no. 4, pp. 855–863, 2001.
- [4] M. Sheikholeslami, D. D. Ganji, and M. M. Rashidi, "Magnetic field effect on unsteady nanofluid flow and heat transfer using Buongiorno model," *J. Magn. Magn. Mater.*, 2016.
- [5] M. Hatami, M. Jafaryar, J. Zhou, and D. Jing, "Investigation of engines radiator heat recovery using different shapes of nanoparticles in H_2O/CH_3OH -based nanofluids," *Int. J. Hydrogen Energy*, vol. 42, no. 16, 2017.
- [6] O. Torsater, B. Engeset, L. Hendraningrat, and S. Suwarno, "Improved Oil Recovery by Nanofluids Flooding: An Experimental Study," in *SPE Kuwait International Petroleum Conference and Exhibition*, 2012.
- [7] L. Levidow, D. Zaccaria, R. Maia, E. Vivas, M. Todorovic, and A. Scardigno, "Improving water-efficient irrigation: Prospects and difficulties of innovative practices," *Agric. Water Manag.*, 2014.
- [8] W. Yu, D. M. France, J. L. Routbort, and S. U. S. Choi, "Review and Comparison of Nanofluid Thermal Conductivity and Heat Transfer Enhancements," *Heat Transf. Eng.*, vol. 29, no. 5, pp. 432–460, 2008.
- [9] S. U. S. Choi and J. A. Eastman, "Thermal Conductivity of Fluids With Pdf," *American Society of Mechanical Engineers*. pp. 99–105, 1995.
- [10] U. Khan, N. Ahmed, and S. T. Mohyud-Din, "Numerical investigation for three dimensional squeezing flow of nanofluid in a rotating channel with lower stretching wall suspended by carbon nanotubes," *Appl. Therm. Eng.*, vol. 113, pp. 1107–1117, 2017.
- [11] Y. J. Hwang *et al.*, "Investigation on characteristics of thermal conductivity enhancement of nanofluids," *Curr. Appl. Phys.*, vol. 6, no. 6 SPEC. ISS., pp. 1068–1071, 2006.
- [12] W. Jiang, G. Ding, H. Peng, Y. Gao, and K. Wang, "Experimental and model research on nanorefrigerant thermal conductivity," *HVAC&R Res.*, vol. 15, no. 3, pp. 651–669, 2009.
- [13] M. Sheikholeslami, D. D. Ganji, M. Gorji-Bandpy, and S. Soleimani, "Magnetic field effect on nanofluid flow and heat transfer using KKL model," *J. Taiwan Inst. Chem. Eng.*, 2014.
- [14] S. Hassani, R. Saidur, S. Mekhilef, and A. Hepbasli, "International Journal of Heat and Mass Transfer A new correlation for predicting the thermal conductivity of nanofluids; using dimensional analysis," *Int. J. Heat Mass Transf.*, vol. 90, pp. 121–130, 2015.
- [15] V. Lee, C. H. Wu, Z. X. Lou, W. L. Lee, and C. W. Chang, "Divergent and Ultrahigh Thermal Conductivity in Millimeter-Long Nanotubes," *Phys. Rev. Lett.*, 2017.
- [16] F. Krahl, A. Giri, J. A. Tomko, T. Tynell, P. E. Hopkins, and M. Karppinen, "Thermal Conductivity Reduction at Inorganic-Organic Interfaces: From Regular Superlattices to Irregular Gradient Layer Sequences," *Advanced Materials Interfaces*, 2018.
- [17] X. Zhao, C. Huang, Q. Liu, I. I. Smalyukh, and R. Yang, "Thermal conductivity model for nanofiber networks," *J. Appl. Phys.*, 2018.
- [18] X. Q. Wang and A. S. Mujumdar, "A review on nanofluids - Part II: Experiments and applications," *Brazilian Journal of Chemical Engineering*, vol. 25, no. 4, pp. 631–648, 2008.
- [19] L. Mohammed, H. G. Gomaa, D. Ragab, and J. Zhu, "Magnetic nanoparticles for environmental and biomedical applications: A review," *Particuology*, vol. 30, pp. 1–14, 2017.
- [20] M. R. Islam, B. Shabani, and G. Rosengarten, "Electrical and Thermal Conductivities of 50/50 Water-ethylene Glycol Based TiO₂ Nanofluids to be Used as Coolants in PEM Fuel Cells," in *Energy Procedia*, 2017, vol. 110, pp. 101–108.
- [21] R. Ul Haq, S. Nadeem, Z. H. Khan, and N. F. M. Noor, "Convective heat transfer in MHD slip flow over a stretching surface in the presence of carbon nanotubes," *Phys. B Condens. Matter*, vol. 457, pp. 40–47, 2015.
- [22] K. J. Zwick, P. S. Ayyaswamy, and I. M. Cohen, "16.Oscillatory enhancement of the squeezing flow of yield stress fluids: a novel experimental result," *J. Fluid Mech.*, vol. 339, pp. 77–87, 1997.
- [23] J. S. Kim, A. Adamcakova-Dodd, P. T. O'Shaughnessy, V. H. Grassian, and P. S. Thorne, "Effects of copper nanoparticle exposure on host defense in a murine pulmonary infection model," *Part. Fibre Toxicol.*, 2011.
- [24] D. R. Baer, D. J. Gaspar, P. Nachimuthu, S. D. Techane, and D. G. Castner, "Application of surface chemical analysis tools for characterization of nanoparticles," *Analytical and Bioanalytical Chemistry*. 2010.
- [25] R. J. Macfarlane, B. Lee, M. R. Jones, N. Harris, G. C. Schatz, and C. A. Mirkin, "Nanoparticle superlattice engineering with DNA," *Science (80-)*, 2011.
- [26] Y. Lu, S. K. Das, S. S. Moganty, and L. A. Archer, "Ionic liquid-nanoparticle hybrid electrolytes and their application in secondary lithium-metal batteries," *Adv. Mater.*, 2012.
- [27] S. L. Pal, U. Jana, P. K. Manna, G. P. Mohanta, and R. Manavalan, "Nanoparticle: An overview of preparation and characterization," *J. Appl. Pharm. Sci.*, 2011.
- [28] A. F. Wibisono, Y. Addad, and J. I. Lee, "A CFD assessment for mixed convection of nanofluids for nuclear application," in *International Conference on Nuclear Engineering, Proceedings, ICONE*, 2015, vol. 2015-Janua.
- [29] K. V. Wong and O. De Leon, "Applications of nanofluids: Current and future," *Advances in Mechanical Engineering*, vol. 2010. 2010.
- [30] W. Anderson, D. Kozak, V. A. Coleman, Å. K. Jämting, and M. Trau, "A comparative study of submicron particle sizing platforms: Accuracy, precision and resolution analysis of polydisperse particle size distributions," *J. Colloid Interface Sci.*, 2013.
- [31] A. M. Siddiqui, S. Irum, and A. R. Ansari, "Unsteady squeezing flow of a viscous MHD fluid between parallel plates, a solution using the homotopy perturbation method," *Math. Model. Anal.*, vol. 13, no. 4, pp. 565–576, 2008.
- [32] R. Dharmalingam, R. Kandasamy, and K. K. Sivagnana Prabhu, "Lorentz forces and nanoparticle shape on water based Cu, Al₂O₃ and SWCNTs," *J. Mol. Liq.*, vol. 231, pp. 663–672, 2017.
- [33] R. Kandasamy, R. Dharmalingam, and K. K. S. Prabhu, "Thermal and solutal stratification on MHD nanofluid flow over a porous vertical plate," *Alexandria Eng. J.*, vol. 57, no. 1, pp. 121–130, 2018.
- [34] P. Singh and M. Kumar, "Mass transfer in MHD flow of alumina water nanofluid over a flat plate under slip conditions," *Alexandria Eng. J.*, vol. 54, no. 3, pp. 383–387, 2015.
- [35] U. Khan, N. Ahmed, Z. A. Zaidi, M. Asadullah, and S. T. Mohyud-Din, "MHD squeezing flow between two infinite plates," *Ain Shams Eng. J.*, vol. 5, no. 1, pp. 187–192, 2014.
- [36] R. Kandasamy, N. A. bt Adnan, and R. Mohammad, "Nanoparticle shape effects on squeezed MHD flow of water based Cu, Al₂O₃ and SWCNTs over a porous sensor surface," *Alexandria Eng. J.*, 2016.

NOMENCLATURE

B_0	Flux density for the magnetic $kg s^{-2} A^1$,	Greek symbols and subscripts	
A, B	Non-negative constant s^{-1}	α	Thermal diffusivity $m^2 s^{-1}$,
C	Volume fraction of the nanoparticle K ,	β	Thermal expansion coefficient
C_w	Volume fraction of the wall nanoparticle K ,	K^{-1}	Density of the base fluid, $kg m^{-3}$,
C_∞	Volume fraction far away from the wall nanoparticle K ,	ρ	Heat capacitance of the nanofluid $J k m^2 K^{-1}$,
$C_{\infty,0}$	Volume fraction due to stratification of the nanoparticle K ,	ρc_p	Electrical conductivity $\Omega^{-1} m^{-1}$,
c_p	Specific heat at constant pressure $J k g^{-1} K^{-1}$,	σ	Dynamic viscosity of the base fluid $kg m^{-1} m^{-1} s^{-1}$,
D_B	Specific diffusivity $m^2 s^{-1}$, a	μ	Thermal stratification parameter, $\frac{4Ax}{T_{\infty} - T_{\infty,0}} = \frac{4A}{m} \left(\frac{s^{-1}}{s^{-1}} \right)$
D_T	Thermophoresis diffusion coefficient, $m^2 s^{-1}$,	ϵ_1	Solutal stratification parameter, $\frac{4Bx}{C_{\infty} - C_{\infty,0}} = \frac{4B}{m} \left(\frac{s^{-1}}{s^{-1}} \right)$
K	Permeability of the porous medium m^2 ,	ϵ_2	Porous parameter, $\frac{x^2}{k R a_x^2} \left(\frac{m^2}{m^2} \right)$
k	Thermal conductivity of the base fluid $kg m s^{-2} K^{-1}$,	ν	Dynamic viscosity, $m^2 s^{-1}$
Le	Lewis number, $\frac{v}{D_B} \left(\frac{m^2 s^{-1}}{m^2 s^{-1}} \right)$	λ	Porous parameter, $\frac{v_f L}{k u_w} \left(\frac{m^2 s^{-1} m}{m m^2 s^{-1}} \right)$
M	Magnetic parameter, $\frac{\sigma B_0^2 L^2}{\mu R a_x^2} \left(\frac{a^{-1} m^1 (kg s^2 A^1)^2 m^2}{kg m^{-1} s^1} \right)$	Ω	Resistance $kg m^2 s^{-3} A^{-2}$,
Nb	Brownian motion parameter $\frac{(pc)_p D_B (C_{\infty} - C_{\infty,0})}{(pc)_f \alpha} \left(\frac{J m^{-3} k^{-1} m^2 s^{-1}}{kg m^{-3} k^{-1} k k} \right)$	Ψ	Dimensionless stream function
Nr	Buoyancy ratio, $\frac{(p_p - p_f \infty)(C_{\infty} - C_{\infty,0})}{p_f \infty \beta (T_{\infty} - T_{\infty,0})(1 - C_{\infty,0})} \left(\frac{kg m^{-3} k}{kg m^{-3} k^{-1} k k} \right)$	η	Similarity variable
Nt	Thermophoresis parameter, $\frac{(pc)_p D_T (T_{\infty} - T_{\infty,0})}{(pc)_f \alpha T_{\infty,0}} \left(\frac{J m^{-3} k^{-1} m^2 s^{-1} k}{J m^{-3} k^{-1} m^2 s^{-1} k} \right)$	f	Dimensionless stream function
Pr	Prandtl number $\frac{v}{\alpha} = \left(\frac{m^2 s^{-1}}{m^2 s^{-1}} \right)$	θ, φ	Dimensionless stream function
T	Temperature of the fluid K ,	γ	Volume fraction
T_w	Temperature of the wall K ,		
T_∞	The temperature of the fluid far away from the wall K ,		
$T_{\infty,0}$	The temperature of the fluid due to stratification K ,		
$x; y$	Stream wise coordinate and cross-stream coordinate m ,		
$u; v$	Velocity components in x and y direction $m s^{-1}$,		
V_0	Velocity of suction/injection $m s^{-1}$,		